



Stage related metabolic profile of the synovial fluid in patients with acute flares of knee osteoarthritis

Delia-Corina Bocsa¹, Carmen Socaciu^{2,3}, Stefania D. Iancu⁴, Michael Andrei Pelea¹, Roxana Ioana Gutiu¹, Nicolae Leopold⁴, Daniela Fodor¹

1) 2nd Internal Medicine Department, Iuliu Hatieganu University of Medicine and Pharmacy, Cluj-Napoca, Romania

2) Faculty of Food Science and Technology, University of Agricultural Sciences and Veterinary Medicine, Cluj-Napoca, Romania

3) BIODIATECH - Research Center for Applied Biotechnology in Diagnosis and Molecular Therapy, Cluj-Napoca, Romania

4) Faculty of Physics, Babeş-Bolyai University, Cluj-Napoca, Romania

Abstract

Background and aim. Osteoarthritis (OA) is the most common joint condition and the leading cause of pain and disability in elderly patients. Currently, there is no biomarker available for the early diagnosis of OA, and limited data is available regarding the molecular basis of progression for OA. For this reason, this study aimed to identify the metabolomic profile of early and late OA using high-performance liquid chromatography coupled with untargeted mass spectrometry (LC-MS).

Methods. 31 patients with knee OA and joint effusion were enrolled. Based on Kellgren/Laurence scale, 12 patients were classified as early OA (eOA) and 19 as late OA (IOA). The synovial fluid (SF) was collected and characterized by untargeted LC-MS. Only the metabolites identified in more than 25% of each group were kept for further analysis. Principal component analysis (PCA) enabled the unsupervised clustering of the eOA and IOA groups. Further, for classification, the best three principal components (PCs) were used as input for two machine learning algorithms (random forest and naïve Bayes), which were trained to discriminate between the eOA and IOA groups.

Results. 43 metabolites were identified in both eOA and IOA, but after selecting the metabolites present in at least 25% of the patients in each group, the metabolomics analysis yielded a panel of only nine metabolites: four metabolites related to phospholipids (phosphatidylcholine 20:0/18:2 and 18:0/20:2, sphingomyelin, and ceramide), three metabolites belonging to purine metabolites (inosine 5'-phosphate, adenosine thiamine diphosphate, and diadenosine 5',5'-diphosphate), one metabolite was a gonadal steroid hormone (estrone 3-sulfate), and one metabolite represented by heme, with all but ceramide (d18:1/20:0) being enriched in the IOA group. By using as features the best three PCs (PC2, PC8 and PC9), random forest and naïve Bayes machine learning algorithms yielded a classification accuracy of 0.81 and 0.78, respectively.

Conclusion. Our LC-MS analysis of SF from patients with eOA and IOA indicates stage-dependent differences, IOA being associated with a perturbed metabolome of phospholipids, purine metabolites, gonadal steroid hormones (estrone 3-sulfate) and a heme molecule. Specific questions need to be answered regarding the biosynthesis and function of these metabolites in osteoarthritic joints, with the aim of developing new relevant biomarkers and therapeutic strategies.

Keywords: metabolomics, osteoarthritis, synovial fluid, liquid chromatography, mass spectrometry

DOI: 10.15386/mpr-2454

Manuscript received: 15.12.2021

Received in revised form: 27.01.2022

Accepted: 15.02.2022

Address for correspondence:

icbocsa@yahoo.com

This work is licensed under a Creative Commons Attribution-NonCommercial-NoDerivatives 4.0 International License

Background and aim

Osteoarthritis (OA) is the most common joint condition and the main cause of pain and disability in elderly patients [1]. Overall, it touches up to 10% of the population over the age of 60 years, the knee being one of the most affected joints [2].

The diagnosis of OA is established on clinical basis, with the clinical picture usually developing after the appearance of joint structural changes. The severity of the disease is determined through several imaging techniques [3] or by arthroscopy [4], but unfortunately, an early diagnosis is often difficult to make [5,6]. Therefore, there has been a growing interest in identifying the metabolomic signature of OA. It is known by now that changes in the metabolomic profile of the joint environment occur before the genomic or proteomic ones [7]. Consequently, the metabolomic analysis could allow an early diagnosis of OA. Also, a better understanding of the disease pathogenesis might lead to the identification of new therapeutic targets with potentially better outcomes [7,8]. To date, few studies have evaluated the metabolomic joint profile of patients with OA [9]. In addition, the results were confounded by differences in identification techniques (global or a targeted metabolomic profile), study design and the type of analyzed biofluid (urine, serum, synovial fluid etc).

Previous metabolomic studies in OA have analyzed urine [10,11] or serum [12,13], with most studies focusing on the synovial fluid (SF) [5,14–22]. SF is a plasma ultrafiltrate and contains molecules produced by joint tissue cells [15], serving as a lubricant for joint surfaces and as a diffusion medium for nutrients. SF is recognized as the most important biofluid for the evaluation of the metabolomic profile of OA [17], being in direct contact with the joint tissues and thus reflecting the biochemical status of the entire joint.

Up to date, the most commonly used analytical techniques for the evaluation of the metabolomic profile are nuclear magnetic resonance spectroscopy and mass spectrometry (MS). Both technologies provide important structural information on various classes of substances and show high analytical accuracy [23–25], although MS is more sensitive and exhibits a broader coverage of the metabolome. A fundamental principle of MS is the representation of metabolite features in any biological matrix by measurement of the spectrum of signals reflecting the mass to charge ratios (m/z) of their ionization products. MS is usually coupled with chromatographic separation techniques such as gas chromatography or liquid chromatography (LC), with the latter being employed for biofluid analysis with both positive and negative ion detection modes [24]. The studies that used LC-MS for SF evaluation in OA have conducted either a global or targeted metabolomic profiling, in a quest to identify OA specific biomarkers [22] and to better differentiate among OA subgroups and phenotypes [15,26].

In this study, we performed a untargeted metabolomic profiling of SF in patients with knee OA using LC-MS, with the aim of identifying metabolomic signatures associated with early forms of OA.

Methods

Inclusion and exclusion criteria

The SF was collected from consecutive adult patients with knee effusions that attended the 2nd Internal Medicine Department, Cluj-Napoca, from March 2019 till March 2020. All the patients were diagnosed with knee OA based on EULAR criteria [27]. The exclusion criteria were the following: history of joint trauma or surgical interventions in the last three months, intraarticular treatment with corticoids or hyaluronic acid in the previous six weeks, other coexistent inflammatory arthritis, and diabetes. All patients underwent clinical examination by an experienced rheumatologist. Demographic data (history, age, gender, body mass index) and clinical outcomes measures such as the visual analog scale for pain (VAS), and Western Ontario and McMaster University OA Index (WOMAC) scores were collected.

Knee ultrasound (US) was performed for all patients (Samsung RS80). The presence of clinically suspected joint effusion was confirmed using the US. An US-guided arthrocentesis was performed. The SF samples were stored at -80°C until the metabolomic analysis.

The radiologic severity of OA was assessed based on the Kellgren/Lawrence scale (K/L), and the patients were divided into two groups: early OA (eOA) (K/L=1 or 2) and late OA (lOA) (K/L=3 or 4) [3].

The present study was approved by the Faculty of Medicine's Ethical Review Committee (Iuliu Hatieganu University of Medicine and Pharmacy Cluj-Napoca). All patients provided written informed consent.

Sample processing

The SF pH was measured before sample processing, using a pH dipstick (Whatman pH Indicator paper, Cyntia).

From each SF sample, 0.6 mL was filtered and mixed with 1.4 mL mixture of methanol: acetonitrile (1:1) to precipitate proteins. The mixture was vortexed for 20 s and kept at a temperature of -20°C for 24 h. After thawing, the vials were centrifuged at 12.500 g for 10 min, and the supernatant was collected, filtered through 0.2 μm PTFE filters, and transferred to autosampler vials for metabolomic analysis.

LC-MS analysis

The MS analysis was performed with a Bruker Daltonics MaXis Impact spectroscope (Bruker GmbH, Bremen, Germany) coupled to a Thermo Scientific HPLC UltiMate 3000 system on a C18 reverse-phase column (Acquity, UPLC C18 BEH) (5 μm , 2.1 x 75 mm) operated at 25°C and at a flow rate of 0.3 mL/min. The injection volume was 5 mL. The mobile phase was represented by a gradient of eluent A (water containing 0.1% formic acid)

and eluent B (methanol: acetonitrile (1:1) containing 0.1% formic acid). The gradient system consisted of 99% A (min 0), 70% A (min 1), 40% A (min 2), 20% A (min 6), 100% B (min 9-10) followed by 5 min with 99% A. The total running time was 15 min.

The LC-MS parameters were set for a mass range between 50-1000 Da. The fragmentation was done using a positive impact (ESI⁺), the nebulizing gas pressure was set at 2.8 Ba and the drying gas flow was set to 12 L/min at 300°C. Before each chromatographic run, a calibration with sodium formate was done. The instrument control and data processing were performed using the specific software provided by Bruker Daltonics, namely Chromeleon, TofControl 3.2, Hystar 3.2, and Data Analysis 4.2.

Statistics

The demographic and clinical data were analyzed in terms of mean and standard deviation. Student t-test for parametric data and Wilcoxon-Mann-Whitney's U test for nonparametric data were performed using Prism 9 software (GraphPad La Jolla California USA).

Metabolomic data were preprocessed using Data Analysis 4.2. First, the individual total ion chromatograms were registered, transformed to base peak chromatograms and then analyzed using the find molecular features function, yielding a table containing the retention time, the peak areas and intensities, the signal/noise ratio for each component together with its mass-to-charge ratio (m/z). The mean of intensity values and standard deviation for each m/z value were used for the identification of metabolites based on the Human Metabolome and Lipid Maps Databases [28].

Next, only the metabolites identified in at least 25% of the patients in each group were kept for further analysis. Principal component analysis (PCA) was performed with the remaining metabolites to reduce the dimensionality of

the dataset and allow the visualization of the unsupervised clustering of the eOA and IOA groups. To select relevant principal components (PCs) that allowed the discrimination between the eOA and IOA groups, Student t-test was employed. The best 3 PC in terms of p values were used for further analysis. The selected PCs were then used as inputs for two machine learning algorithms (random forest and naïve Bayes), which were trained to discriminate between the eOA and IOA groups. The machine learning algorithms were validated using leave-one-out cross-validation.

The statistical analysis was performed using Quasar-Orange software, Orange-Spectroscopy library (Bioinformatics Laboratory of the University of Ljubljana, Slovenia).

Results

Demographic and clinical data

In this study, SF was collected from 31 patients with knee OA. Based on K/L criteria, a number of 12 patients were diagnosed with eOA, and 19 with IOA. There were significant differences between the two groups in terms of age and body mass index, the IOA patients being significantly older and with higher body mass index (Table I). There were no statistically significant differences in VAS and WOMAC scores between the two groups (Table I). The mean SF pH values were 8.3±0.4 for patients with eOA and 8.2±0.5 for IOA, respectively, with no statistically significant differences between the two groups (Student t-test, p=0.71).

LC-MS identification of metabolites in the SF of eOA and IOA groups

The results of the LC-MS analysis of SF yielded 43 metabolites, (Table II), which were identified based on using the Human Metabolome and Lipid Maps Databases [28].

Table I. Demographic and clinical data of early and late osteoarthritis groups.

Parameter	eOA n=12 (39%)		IOA n=19 (61%)		Significance
RX	Stage 1: n=3 (10%) Stage 2: n=9 (29%)		Stage 3: n=13 (42%) Stage 4: n=6 (19%)		
Gender	Male n=9 (75%)	Female n=3 (25%)	Male n=7 (37%)	Female n=12 (63%)	
Age (years)	62±11		70±7		Student <i>t</i> test, p=0.01
BMI (kg/m ²)	27.5±5.6		32.1±1.42		Mann-Whitney U test, p=0.02
VAS	6.2±1.9		6.4±1.5		Mann-Whitney U test, p=0.8
WOMAC	21.1±5.5		24.4±6.1		Student <i>t</i> test, p=0.2

The results are expressed as number (%) or mean ± standard deviation.

Abbreviations: RX - radiological OA stage, BMI - Body Mass Index, VAS - the visual analog scale for pain, WOMAC - Western Ontario and McMaster University Osteoarthritis Index, eOA - patient group with early osteoarthritis, IOA - patient group with late osteoarthritis.

Table II. The m/z values of metabolites from SF for the early and late osteoarthritis groups.

m/z	Metabolite
239.1694	Pentadecynoic acid (C15:4)
245.0862	1,5-Anhydroglucitol-6-phosphate
247.1380	5,6-Dihydrouridine
271.1964	Heptadecanoic acid
301.1512	Andrenosterone (cortisol metabolite)
349.0022	Inosine 5'-phosphate
350.9995	Estrone 3-sulfate
352.9969	N-Acetyl-7-O-acetylneuraminic acid
353.279	Prostaglandin E2
381.3124	Mycolipenic acid (C25)
455.3544	Lysophosphatidic acid 18:0
496.364	Lysophosphatidylcholine 16:0
499.3724	Oleanolic acid acetate
518.3484	Lysophosphatidylcholine 18:3
520.3662	Lysophosphatidylcholine 18:2
522.382	Lysophosphatidylcholine 18:1
524.3981	Lysophosphatidylcholine 18:0
527.3501	Triradylglycerol (10:0/10:0/8:0)
534.3233	Ceramide (d14:2/20:1)
542.3509	Lysophosphatidylcholine 20:5
544.3689	Lysophosphatidylcholine 20:4
546.3897	Lysophosphatidylcholine 20:3
560.484	Glucosylceramide (d14:1/10:0)
565.3668	Dichloran Glycerol (18:2/14:0/0:0)
566.4596	Ceramide (d18:0/18:1)
572.4038	Ceramide (t18:0/16:0(2OH))
575.4128	Glucosyl 25-hydroxyhexacosanoate
578.512	Ceramide (d16:2/20:1(2OH)) or Ceramide-phosphate (d18:0/13:0)
579.3265	Dichloran Glycerol (33:2)
586.5126	Ceramide (t18:0/17:0(2OH))
587.4087	Behenyl linolenate C40H72O2
588.4993	C8 beta-D-glucosyl N-acyl sphingosine
594.5095	Ceramide (d18:1/20:0)
616.2157	Heme
675.0371	Adenosine thiamine diphosphate
677.0342	Diadenosine 5',5'-diphosphate
679.0318	Ceramide (d18:1/26:0)
679.5549	Cholesterol ester (20:1)
681.03	Ceramide (d18:0/26:0)
701.5544	Sphingomyelin (d18:1/16:1)
782.6255	2,5-Anhydroglucitol
798.6162	PC (P-18:0/20:2)/ PC (P-20:0/18:2)
814.6475	Phosphatidylcholine (20:0/18:2)

Multivariate analysis

After keeping only the metabolites present in at least 25% of the patients in each group, the metabolomics

analysis yielded a panel of 9 metabolites (Table III). The violin plots of mean intensities for the 9 metabolites are presented in figure 1. In total, 8 metabolites were enriched in the IOA group, while one of them was enriched in the eOA group.

Next, PCA was performed on the panel of 9 metabolites and PCs were ranked using the p value of Student t testing between the eOA and IOA groups, with PC2, PC8, and PC9 selected for further analysis.

The score plot for PC2 and PC8 showed a clear tendency of clustering of the two groups (Figure 2A). The loading plots of PC2, PC8, and PC9 highlight the contribution of the metabolites to eOA and IOA clustering (Figure 2B). By correlating the scatter plot with the afferent loading plots, the metabolic differences between eOA and IOA are assessed. PC2 shows the positive correlation of Sphingomyelin (d18:1/16:1), Inosine 5'-phosphate, Phosphatidylcholine (20:0/18:2) and Diadenosine 5',5'-diphosphate, metabolites that show higher levels in IOA patients compared to eOA (Figure 2A). PC8 shows the negative correlation between Phosphatidylcholine (18:0/20:2) and Heme. As observed in the scatter plot, eOA patients are grouped in the negative region of PC8, meaning that they are characterized by a higher level of Heme and a lower level of Phosphatidylcholine (18:0/20:2) when compared to IOA patients. Finally, PC9 highlights the negative correlated contribution from Estrone 3-sulfate and Adenosine thiamine diphosphate in eOA and IOA clustering.

To test the performance of the PC2, PC8 and PC9 in discriminating between the eOA and IOA groups, two machine learning algorithms were used (random forest, and naïve Bayes). Thus, the three previously selected PCs were employed as input for the machine learning algorithms, yielding an AUC of 0.81 for random forest, and 0.78 for Naïve Bayes (Figure 2C). The performance metrics of the two classification algorithms cross-validated by leave-one-out cross-validation technique are presented in Table IV.

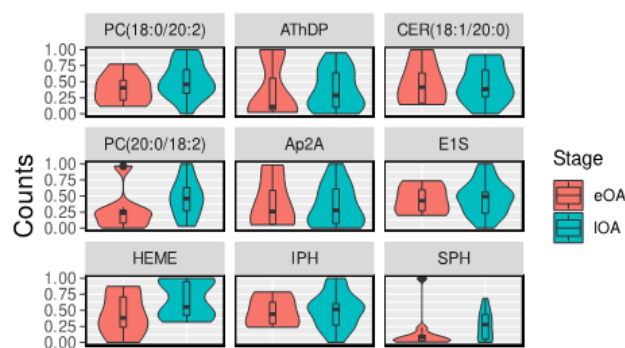


Figure 1. Violin plot of the selected 9 metabolites. **Abbreviations:** HEME – Heme molecule; PC – Phosphatidylcholine; SPH – Sphingomyelin; CER – Ceramide; IPH – Inosine 5'-phosphate; E1S – Estrone 3-sulfate; AthDP – Adenosine thiamine diphosphate; Ap2A – Diadenosine 5',5'-diphosphate.

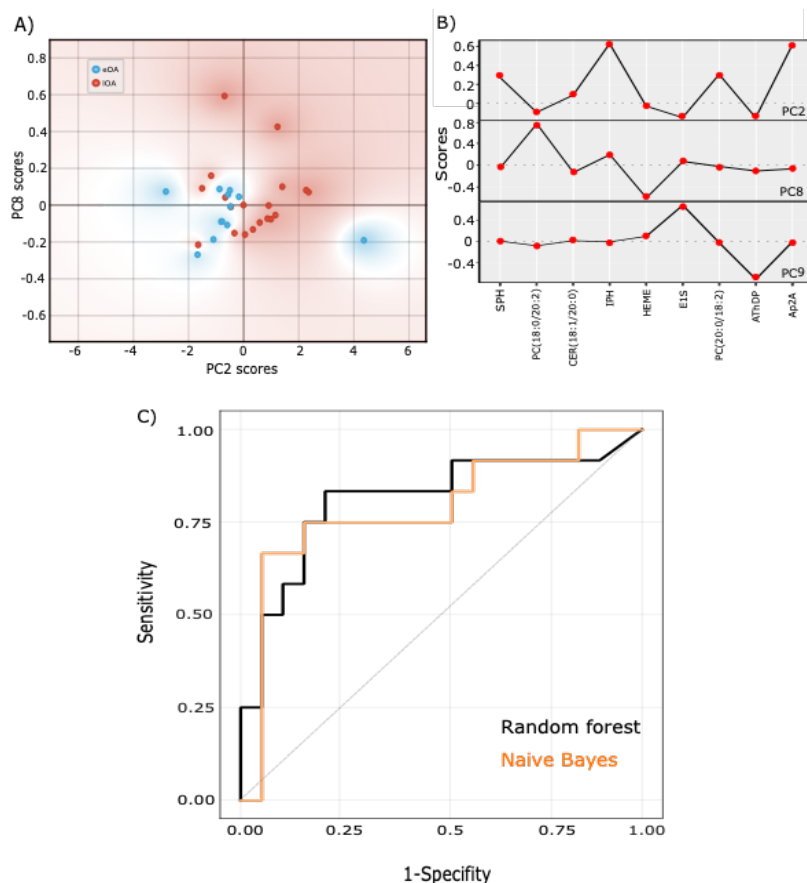


Figure 2. A) The score plots of PC2 and PC8, which were used to assess the clustering of the early and late osteoarthritis groups (eOA vs lOA). B) The loading plots corresponding to PC2, 8, and 9. C) Head-to-head comparison of the receiver operating characteristic (ROC) curves yielded by random forest and naïve Bayes for the discrimination between the eOA and lOA based on PC2, PC8, and PC9. **Abbreviations:** HEME – Heme molecule; PC – Phosphatidylcholine; SPH – Sphingomyelin; CER – Ceramide; IPH – Inosine 5'-phosphate; EIS – Estrone 3-sulfate; AThDP – Adenosine thiamine diphosphate; Ap2A – Diadenosine 5',5'-diphosphate.

Table III. The m/z of the metabolites from synovial fluid used for discriminating between early and late osteoarthritis.

m/z	Metabolite	Student's <i>t</i> -test	
		p value	Adjusted p value
616.2157	Heme	0.188	0.618
814.64755	Phosphatidylcholine (20:0/18:2)	0.224	0.618
701.5544	Sphingomyelin (d18:1/16:1)	0.314	0.647
798.6162	Phosphatidylcholine (18:0/20:2)	0.352	0.647
349.0022	Inosine 5'-phosphate	0.867	0.995
677.0342	Diadenosine 5',5'-diphosphate	0.878	0.995
350.9995	Estrone 3-sulfate	0.878	0.995
594.5095	Ceramide (d18:1/20:0)	0.975	0.995
675.0371	Adenosine thiamine diphosphate	0.995	0.995

Table IV. The performance metrics for the discrimination between early and late osteoarthritis by random forest and naïve Bayes.

Machine learning model	AUC	CA	F1	Precision	Recall
Random forest	0.81	0.80	0.80	0.80	0.80
Naïve Bayes	0.78	0.64	0.64	0.68	0.64

Abbreviations: AUC-area under the curve; CA- classification accuracy; F1-score represents the harmonic mean of precision and recall; Precision- positive predicted values; Recall-sensitivity.

Discussion

In this study, we employed LC-MS for performing an untargeted metabolomic profiling of SF from 31 patients with OA. The results showed that IOA patients were significantly older and with higher body mass index than eOA patients (Table I), in line with previous reports demonstrating that age and obesity are risk factors for OA [29]. Indeed, Deshpande et al. reported the prevalence of symptomatic knee OA increases with every decade of life [30] and a meta-analysis found that the odds ratio for having OA in obese or overweight patients compared with normal-weight individuals was 2.96 [31].

The results of the metabolomic profiling of 31 OA patients yielded 43 metabolites which were identified by comparison with the Human Metabolome and Lipid Maps Databases [28] (Table II), of which only 9 were present in at least 25% of the patients. Among the 9 metabolites, 4 were pertaining to phospholipids (Phosphatidylcholine 20:0/18:2 and 18:0/20:2, Sphingomyelin, and Ceramide), 3 were represented by purine metabolites (Inosine 5'-phosphate, Adenosine thiamine diphosphate, and Diadenosine 5',5'-diphosphate), one metabolite was a gonadal steroid hormone (Estrone 3-sulfate) and one metabolite was represented by Heme, with all but Ceramide (d18:1/20:0) being enriched in the IOA group.

Next, we performed PCA on the 9 metabolites, and selected PC2, PC8 and PC9 for further analysis. PC2 and PC8 showed Sphingomyelin (d18:1/16:1), Inosine 5'-phosphate, Phosphatidylcholine (20:0/18:2) Diadenosine 5',5'-diphosphate and Phosphatidylcholine (18:0/20:2) have higher levels in IOA compared to eOA, while Heme has a higher level in eOA compared to IOA. Based on score values of PC2 and PC8, the eOA and IOA exhibited a good unsupervised clustering, demonstrating the distinct metabolomic landscape of these two groups (Figure 2A).

Using the score values of PC2, PC8 and PC9 as features for machine learning algorithms, eOA and IOA groups are classified with an AUC of 0.81 for random forest, and 0.78 for Naïve Bayes (Figure 2C).

Membrane phospholipid species contribute to boundary lubrication that is provided by SF. Altered levels of lubricants can be associated with increased friction, leading to articular cartilage damage [19]. The higher concentration of phospholipids in the SF of IOA patients was noted for the first time by Kosinska et al., who performed a comparative lipidomic analysis of synovial fluid in human and canine osteoarthritis [32]. In line with our results, the IOA group showed an increase of the median concentration of phospholipids by 4.8 fold compared to the control group, while eOA showed an increase of only 2.8 fold. In another study, the same group reported a higher concentration of phosphatidylcholine and sphingomyelin in the IOA, suggesting that the mechanisms that drive these alterations are related to fibroblast-like synoviocytes, which mediate

the synthesis and release of phospholipids, increasing their production to protect cartilage from friction-induced mechanical damage [19].

Diadenosine 5',5'-diphosphate (Ap2A) is a member of the diadenosine polyphosphates family, which are ubiquitous natural compounds found in a wide variety of prokaryotic and eukaryotic cells that are believed to act as extracellular signaling molecules and regulators of cellular functions [33]. In humans, few data are available regarding its biological function. Pliyev et al., found that Ap2A delays neutrophil apoptosis via the adenosine A2A receptor and cAMP/PKA pathway [34], while in platelets it has a negative modulation effect on aggregation [35]. It is worth mentioning that mice lacking adenosine A2A receptors develop spontaneous OA by 16 weeks of age [36], but there is no data regarding Ap2A function in OA disease.

Inosine 5'-phosphate is a precursor of inosine, a product of adenosine breakdown [37]. Previous studies demonstrated that the nucleoside adenosine and its metabolite inosine exert anti-inflammatory effects in different tissues in the human body, such as the lung, liver, kidney and joints, after binding to specific G protein-coupled adenosine receptors (like adenosine A2A receptors) [38]. Traditionally OA has been considered to be caused by mechanical cartilage breakdown. However, it is now well-accepted that inflammation plays a critical role in the disease progression in cartilage and the synovium, as OA displays a low-grade chronic inflammation, primarily mediated by innate immunity [39]. The role of adenosine/inosine as an intrinsic anti-inflammatory mechanism in joint inflammation is not clear, and further studies are required [38].

Estrone 3-sulfate (E1S) is an endogenous steroid and an estrogen ester that can be transformed into estrone and estrogen. Estrogen levels regulate changes in OA by inhibiting degradation of the extracellular matrix, estrogen deficiency resulting in resorption of subchondral bone and degeneration of articular cartilage [40]. E1S is a major source of local bioactive estrogen formation, the osteoblast being equipped with steroid sulfatase enzymes (STS) that can convert E1S into estrone and estradiol [41]. Limited data regarding STS activity and the role of E1S in bones are available, but Dias et al. reported an insightful study regarding the role of STS and E1S in stimulating cell proliferation and growth of osteoblastic cells in cultures [42]. Whether our results pointing to high levels of E1S are a sign of compensatory activity of osteoblast, or an accumulation of estrogen substrate because of low STS activity is unknown, and further studies are required.

Heme is a ubiquitous molecule composed of an atom of iron coordinated by the four-pyrrole ring of protoporphyrin IX, and is also the precursor and degradation product of hemoglobin [43]. Heme has a variety of roles like co-factor for cytochromes involved in the mitochondrial electron transport chain, oxygen transporters

(e.g. hemoglobin, neuroglobin), heme-using peroxidases (e.g. catalase), and nitric oxide synthases and is associated with oxidative stress and degenerative processes [43,44]. Heme is endogenously synthesized in the mitochondria from succinyl-CoA and glycine and is degraded by Heme oxygenase-1 (HO-1). This is of particular interest because the HO-1 expression decreases with aging in articular cartilages and menisci of mouse knees [44], and might explain why the IOA group had higher levels of Heme since IOA group was significantly older than eOA (Table I). Further studies evaluating this hypothesis are needed.

An important limitation of this study is represented by the relatively small number of patients and the lack of the validation of the metabolites by quantitative MS. From a translational point of view, it would also be interesting to assess whether the findings from the SF can also be extrapolated to other biofluids that are more readily available, such as urine, saliva or serum. Future studies concerned with the metabolomic profiling of OA patients should also complement metabolomics by mechanistic studies, which might lead to novel insights regarding the roles of metabolome in the onset and development of OA, with the ultimate goal of pinpointing druggable targets that can be modulated pharmacologically by disease-modifying agents. Also, other joint seats should be investigated, given that our study focused solely on knee OA.

Conclusion

The results of this metabolomic study concerned with the SF showed that IOA is associated with a perturbed metabolome in terms of phospholipids (Phosphatidylcholine 20:0/18:2 and 18:0/20:2, Sphingomyelin, and Ceramide), purine metabolites (Inosine 5'-phosphate, Adenosine thiamine diphosphate, and Diadenosine 5',5'-diphosphate), gonadal steroid hormone (Estrone 3-sulfate) and Heme, with all but Ceramide (d18:1/20:0) being enriched in the IOA group. More studies delineating the molecular mechanisms underlying these observations are needed in order to translate these findings into clinically relevant biomarkers and therapeutic strategies.

Acknowledgements

N.L. and SDI highly acknowledge support from the Romanian Ministry of Research and Innovation, CCCDI-UEFISCDI, project number PN-III-P2-2.1-PED-2019-3268.

References

1. Neogi T. The epidemiology and impact of pain in osteoarthritis. *Osteoarthritis Cartilage*. 2013;21:1145–1153.
2. Panikkar M, Attia E, Dardak S. Osteoarthritis: A Review of Novel Treatments and Drug Targets. *Cureus*. 2021;13:e20026.
3. Kellgren JH, Lawrence JS. Radiological assessment of osteo-arthrosis. *Ann Rheum Dis*. 1957;16:494–502.
4. Slattery C, Kweon CY. Classifications in Brief: Outerbridge Classification of Chondral Lesions. *Clin Orthop Relat Res*. 2018;476:2101–2104.
5. Carlson AK, Rawle RA, Adams E, Greenwood MC, Bothner B, June RK. Application of global metabolomic profiling of synovial fluid for osteoarthritis biomarkers. *Biochem Biophys Res Commun*. 2018;499:182–188.
6. Mobasher A. Osteoarthritis year 2012 in review: biomarkers. *Osteoarthritis Cartilage*. 2012;20:1451–1464.
7. Adams SB Jr, Setton LA, Kensicki E, Bolognesi MP, Toth AP, Nettles DL. Global metabolic profiling of human osteoarthritic synovium. *Osteoarthritis Cartilage*. 2012;20:64–67.
8. Li JT, Zeng N, Yan ZP, Liao T, Ni GX. A review of applications of metabolomics in osteoarthritis. *Clin Rheumatol*. 2021;40:2569–2579.
9. Ruiz-Romero C, Rego-Perez I, Blanco FJ. What did we learn from “omics” studies in osteoarthritis. *Curr Opin Rheumatol*. 2018;30:114–120.
10. Abdelrazig S, Ortori CA, Doherty M, Valdes AM, Chapman V, Barrett DA. Metabolic signatures of osteoarthritis in urine using liquid chromatography-high resolution tandem mass spectrometry. *Metabolomics*. 2021;17:29.
11. Lamers RJ, van Nesselrooij JH, Kraus VB, Jordan JM, Renner JB, Dragomir AD, et al. Identification of an urinary metabolite profile associated with osteoarthritis. *Osteoarthritis Cartilage*. 2005;13:762–768.
12. Zhang W, Sun G, Likhodii S, Liu M, Aref-Eshghi E, Harper PE, et al. Metabolomic analysis of human plasma reveals that arginine is depleted in knee osteoarthritis patients. *Osteoarthritis Cartilage*. 2016;24:827–834.
13. Xu B, Su H, Wang R, Wang Y, Zhang W. Metabolic networks of plasma and joint fluid base on differential correlation. *PLoS One*. 2021;16:e0247191.
14. Akhbari P, Jaggard MK, Boulangé CL, Vaghela U, Graça G, Bhattacharya R, et al. Differences in the composition of hip and knee synovial fluid in osteoarthritis: a nuclear magnetic resonance (NMR) spectroscopy study of metabolic profiles. *Osteoarthritis Cartilage*. 2019;27:1768–1777.
15. Carlson AK, Rawle RA, Wallace CW, Brooks EG, Adams E, Greenwood MC, et al. Characterization of synovial fluid metabolomic phenotypes of cartilage morphological changes associated with osteoarthritis. *Osteoarthritis Cartilage*. 2019;27:1174–1184.
16. Hügler T, Kovacs H, Heijnen IA, Daikeler T, Baisch U, Hicks JM, et al. Synovial fluid metabolomics in different forms of arthritis assessed by nuclear magnetic resonance spectroscopy. *Clin Exp Rheumatol*. 2012;30:240–245.
17. Kim S, Hwang J, Kim J, Ahn JK, Cha HS, Kim KH. Metabolite profiles of synovial fluid change with the radiographic severity of knee osteoarthritis. *Joint Bone Spine*. 2017;84:605–610.
18. Kosinska MK, Liebisch G, Lochner G, Wilhelm J, Klein H, Kaesser U, et al. Sphingolipids in human synovial fluid - a lipidomic study. *PLoS One*. 2014;9:e91769.

19. Kosinska MK, Liebisch G, Lochnit G, Wilhelm J, Klein H, Kaesser U, et al. A lipidomic study of phospholipid classes and species in human synovial fluid. *Arthritis Rheum.* 2013;65:2323–2333.
20. Mickiewicz B, Heard BJ, Chau JK, Chung M, Hart DA, Shrive NG, et al. Metabolic profiling of synovial fluid in a unilateral ovine model of anterior cruciate ligament reconstruction of the knee suggests biomarkers for early osteoarthritis. *J Orthop Res.* 2015;33:71–77.
21. Mickiewicz B, Kelly JJ, Ludwig TE, Weljie AM, Wiley JP, Schmidt TA, et al. Metabolic analysis of knee synovial fluid as a potential diagnostic approach for osteoarthritis. *J Orthop Res.* 2015;33:1631–1638.
22. Zheng K, Shen N, Chen H, Ni S, Zhang T, Hu M, et al. Global and targeted metabolomics of synovial fluid discovers special osteoarthritis metabolites. *J Orthop Res.* 2017 Sep 1;35(9):1973–81.
23. Lindon JC, Nicholson JK. Spectroscopic and statistical techniques for information recovery in metabolomics and metabolomics. *Annu Rev Anal Chem (Palo Alto Calif).* 2008;1:45–69.
24. Akhbari P, Karamchandani U, Jaggard MKJ, Graça G, Bhattacharya R, Lindon JC, et al. Can joint fluid metabolic profiling (or “metabonomics”) reveal biomarkers for osteoarthritis and inflammatory joint disease? *Bone Joint Res.* 2020;9:108–119.
25. Lu W, Su X, Klein MS, Lewis IA, Fiehn O, Rabinowitz JD. Metabolite Measurement: Pitfalls to Avoid and Practices to Follow. *Annu Rev Biochem.* 2017;86:277–304.
26. Zhang W, Likhodii S, Zhang Y, Aref-Eshghi E, Harper PE, Randell E, et al. Classification of osteoarthritis phenotypes by metabolomics analysis. *BMJ Open.* 2014;4:e006286.
27. Zhang W, Doherty M, Peat G, Bierma-Zeinstra MA, Arden NK, Bresnihan B, et al. EULAR evidence-based recommendations for the diagnosis of knee osteoarthritis. *Ann Rheum Dis.* 2010;69:483–489.
28. Wishart DS, Knox C, Guo AC, Eisner R, Young N, Gautam B, et al. HMDB: a knowledgebase for the human metabolome. *Nucleic Acids Res.* 2009;37(Database issue):D603–D610.
29. Musumeci G, Aiello FC, Szychlinska MA, Di Rosa M, Castrogiovanni P, Mobasher A. Osteoarthritis in the XXIst century: risk factors and behaviours that influence disease onset and progression. *Int J Mol Sci.* 2015;16:6093–6112.
30. Deshpande BR, Katz JN, Solomon DH, Yelin EH, Hunter DJ, Messier SP, et al. Number of Persons with Symptomatic Knee Osteoarthritis in the US: Impact of Race and Ethnicity, Age, Sex, and Obesity. *Arthritis Care Res (Hoboken).* 2016;68:1743–1750.
31. Blagojevic M, Jinks C, Jeffery A, Jordan KP. Risk factors for onset of osteoarthritis of the knee in older adults: a systematic review and meta-analysis. *Osteoarthritis Cartilage.* 2010;18:24–33.
32. Kosinska MK, Mastbergen SC, Liebisch G, Wilhelm J, Dettmeyer RB, Ishaque B, et al. Comparative lipidomic analysis of synovial fluid in human and canine osteoarthritis. *Osteoarthritis Cartilage.* 2016;24:1470–1478.
33. Park HS, Hourani SM. Differential effects of adenine nucleotide analogues on shape change and aggregation induced by adenosine 5-diphosphate (ADP) in human platelets. *Br J Pharmacol.* 1999;127:1359–1366.
34. Pliyev BK, Dimitrieva TV, Savchenko VG. Diadenosine diphosphate (Ap₂A) delays neutrophil apoptosis via the adenosine A_{2A} receptor and cAMP/PKA pathway. *Biochem Cell Biol.* 2014;92:420–424.
35. Magnone M, Basile G, Bruzzese D, Guida L, Signorello MG, Chothi MP, et al. Adenylic dinucleotides produced by CD38 are negative endogenous modulators of platelet aggregation. *J Biol Chem.* 2008;283:24460–24468.
36. Castro CM, Corciulo C, Friedman B, Li Z, Jacob S, Fenyo D, et al. Adenosine A_{2A} receptor null chondrocyte transcriptome resembles that of human osteoarthritic chondrocytes. *Purinergic Signal.* 2021;17:439–448.
37. Yin J, Ren W, Huang X, Deng J, Li T, Yin Y. Potential Mechanisms Connecting Purine Metabolism and Cancer Therapy. *Front Immunol.* 2018;9:1697.
38. Sohn R, Junker M, Meurer A, Zaucke F, Straub RH, Jenei-Lanzl Z. Anti-Inflammatory Effects of Endogenously Released Adenosine in Synovial Cells of Osteoarthritis and Rheumatoid Arthritis Patients. *Int J Mol Sci.* 2021;22:8956.
39. Gratal P, Lamuedra A, Medina JP, Bermejo-Álvarez I, Largo R, Herrero-Beaumont G, et al. Purinergic System Signaling in Metainflammation-Associated Osteoarthritis. *Front Med (Lausanne).* 2020;7:506.
40. Xu X, Li X, Liang Y, Ou Y, Huang J, Xiong J, et al. Estrogen Modulates Cartilage and Subchondral Bone Remodeling in an Ovariectomized Rat Model of Postmenopausal Osteoarthritis. *Med Sci Monit.* 2019;25:3146–3153.
41. Muir M, Romalo G, Wolf L, Elger W, Schweikert HU. Estrone sulfate is a major source of local estrogen formation in human bone. *J Clin Endocrinol Metab.* 2004;89:4685–4692.
42. Dias NJ, Selcer KW. Steroid sulfatase mediated growth of human MG-63 pre-osteoblastic cells. *Steroids.* 2014;88:77–82.
43. Chiabrando D, Fiorito V, Petrillo S, Bertino F, Tolosano E. HEME: a neglected player in nociception? *Neurosci Biobehav Rev.* 2021;124:124–136.
44. Takada T, Miyaki S, Ishitobi H, Hirai Y, Nakasa T, Igarashi K, et al. Bach1 deficiency reduces severity of osteoarthritis through upregulation of heme oxygenase-1. *Arthritis Res Ther.* 2015;17:285.